Nanoscale

Accepted Manuscript

This article can be cited before page numbers have been issued, to do this please use: E. Dalcanale, N. Bontempi, E. Biavardi, D. Bordiga, G. Candiani, I. Alessandri and P. Bergese, *Nanoscale*, 2017, DOI: 10.1039/C7NR02491F.

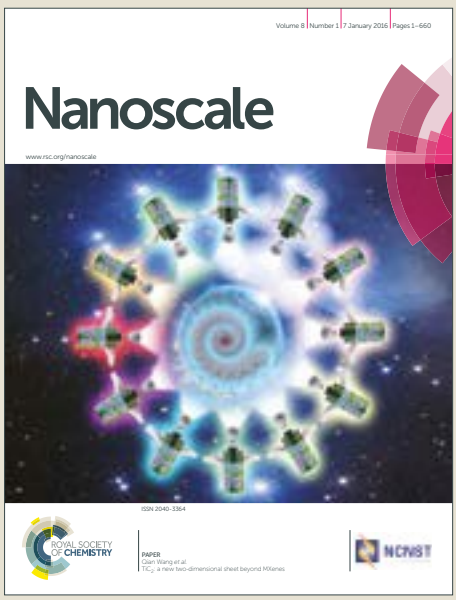

ROYAL SOCIETY OF CHEMISTRY

rsc.li/nanoscale

View Article Online
DOI: 10.1039/C7NR02491F

Nanoscale

ARTICLE

Probing lysine mono-methylation in histone H3 tail peptides with an abiotic receptor coupled to a non-plasmonic resonator

Received 00th January 20xx,
Accepted 00th January 20xx

DOI: 10.1039/x0xx00000x

www.rsc.org/

N. Bontempi,[a] E. Biavardi,[b] D. Bordiga,[c] G. Candiani,[d] I. Alessandri,[a]* P. Bergese[c]* and E. Dalcanale[b]*

Binder and effector molecules that allow studying and manipulating epigenetic processes are of biological relevance and pose severe technical challenges. We report the first example of a synthetic receptor able to recognize mono-methylated lysines in a histone H3 tail peptide, which has relevant function in epigenetic regulation. Recognition is robust and specific regardless the position and the number of the mono-methylated lysines along the polypeptide chain. The peptide is first captured in solution by a tetraphosphonate cavitand (**Tiiii**) that selectively bind its Lys-NMe$^+$ moieties. Separation from solution and detection of the peptide-**Tiiii** complexes is then enabled in one single step by an all dielectric SiO_2-TiO_2 core-shell resonators (T-rex), which captures the complex and operates fully reproducible signal transduction by non-plasmonic surface enhanced Raman scattering (SERS) without degrading the complex. The realized abiotic probe is able to distinguish multiple mono-methylated peptides from the single mono-methylated ones.

Introduction

Post-translational modifications (PTMs), such as histone lysine methylation, are a fundamental part of the histone code, which have a large influence on gene expression.[1-5] Histones have cationic amino-terminal tails (-NH_3^+) that are subjected to several PTMs, such as the mono-methylation of the ε-amine of lysines. Sequencing studies have shown that several lysines of the histone H3 tail peptide (e.g. H3K4, H3K9, H3K20 and H3K27) are often the preferred methylation sites, although species-specific differences do exist.[6] Even though epigenetic alterations have sparked great interest, for example into deciphering the regulatory pathways and function of histone PTMs in cancer and type 2 diabetes,[7,8] the mono-methylation of lysine is unfortunately a very challenging moiety to identify and measure. Indeed, the relatively low molecular weight of the methyl residue and the lack of a significant charge difference between monomethylated and non-methylated lysine *de facto* exclude detection via direct physicochemical methods. Besides, developing robust antibodies capable of targeting lysine methylation with little or no dependence on the local amino acid sequence has been proven very difficult.[1] This unmet need has severely hampered the study of the histone, and protein in general, methylome and its medical translation.

Drawing inspiration from Nature,[9,10] chemists have started to explore the possibility to use synthetic receptors for the recognition of histone methylation.[11-14] So far, most of the attention was given to the complexation of side chain di-methylated[15] and trimethylated[16-18] lysine (Nε), while synthetic receptors that bind selectively monomethylated forms (Lys-NMe$^+$) of the side chains of lysine residues are unprecedented. Tetraphosphonate cavitands (**Tiiii** from now onward)[19,20] (Scheme 1) have an edge in this respect, being the only synthetic receptors known to bind monomethylated amino acids with high selectivity both in water and in organic solvents.[21] The pivotal role played by cation-π interactions[22] of the acidic $^+NH_2$–CH_3 group with the π-basic cavity strongly coupled to the steric demand for inclusion favors monomethylated ammonium ions versus pristine, di- and trimethylated ammonium ions.[23]

Post-translational modifications in proteins are mainly detected using indicator displacement assays.[11,24,25] Recently, this methodology has been proposed for the detection of trimethylated lysine in the H3 histone tail using a deep cavitand as recognition element.[26] In view of separation and biosensing applications, solid phase supported methods able for capturing, transduction and amplification with high fidelity and reproducibility are needed. In this regard, surface Raman spectroscopy represents a powerful resource. Metal nanoparticle (NP) substrates with a plasmonic resonance in the UV-Vis-NIR (*e.g.* Al, Ag, Au, Cu) are typically utilized to enhance the Raman response of most of the analytes characterized by a very low-cross section, taking advantage of the plasmon-driven

[a] Department of Mechanical and Industrial Engineering, Chemistry for Technologies Laboratory, University of Brescia and INSTM UdR Brescia, Via Branze 38, 25123 Brescia, Italy. E-mail: ivano.alessandri@unibs.it
[b] Department of Chemistry, Life science and Environmental Sustainability, University of Parma and INSTM UdR Parma, Parco Area delle Scienze 17/A, 43124 Parma, Italy. E-mail: enrico.dalcanale@unipr.it
[c] Department of Molecular and Translational Medicine, University of Brescia and INSTM UdR Brescia, Viale Europa 11, 25123 Brescia, Italy. E-mail: paolo.bergese@unibs.it
[d] Department of Chemistry, Materials and Chemical Engineering "G. Natta, Polytechnic of Milan and INSTM UdR Milano, Via Mancinelli 7, 20131 Milano, Italy
[e]

Electronic Supplementary Information (ESI) available: Peptide structure and molecular minimization; ^{31}P and ^1H-NMR titration of peptides with cavitand. See DOI: 10.1039/x0xx00000x

SERS effect). However, SERS detection is often affected by huge increase of the local electromagnetic field (the so-called instability of the Raman signals and low reproducibility, due to the heavy perturbation of the system under analysis caused by the excited plasmonic NPs, which generate local heating and catalyze unwanted photo-reactions. For this reason, the weak interactions that hold a mono-methylated lysine-**Tiiii** complex would hardly survive plasmonic SERS and be quickly degraded. We recently circumvented this drawback by coupling **Tiiii** receptors to all-dielectric resonators made of SiO_2/TiO_2 core/shell (T-rex) colloids.[27] The T-rex beads exploit the synergistic combination of the evanescent fields resulting from total internal reflection and multiple scattering of light at the bead-to-bead interface for amplifying the optical path length and extracting more Raman photons, without altering the stability of the analytes.[28-31]

In this work we contemporarily assess the ability of **Tiiii** as specific binder for monomethylated histone H3 tail peptides and proof that all-dielectric enhanced Raman spectroscopy by T-rex is the suitable mean for enabling separation and transduction of the peptide-**Tiiii** complexes.

Experimental

Peptide structure and molecular minimization (Scheme 1). Fluorenylmethyloxycarbonyl (FMOC)-protected reference histone (PC: Fmoc-RTKQTARKSTGGKAP, MW: 1809.07 g/mol, purity: 97.02%), mono-methylated histones (P1: Fmoc-RTK(Me)QTARKSTGGKAP, MW: 1822.83 g/mol, purity: 98.52%; P2: Fmoc-RTKQTARK(Me)STGGKAP, 1823.07 g/mol, purity: 95.35%; P3: Fmoc-RTKQTARKSTGGK(Me)AP, 1823.07 g/mol, purity: 95.60%) and tri-methylated histone (P123: Fmoc-RTK(Me)QTARK(Me)STGGK(Me)AP, 1851.7 g/mol, purity: 99.20%), all sketched in Fig. 1a. Peptides were purchased from ProteoGenix SAS (Schiltigheim, France).

Peptides were first designed using ChemBioDraw Ultra software (Version 12.0, PerkinElmer Informatics, Waltham, MA, USA). Afterwards, they were modeled using the AMBER3 (Assisted Model Building and Energy Refinement, DOI: 10.1002/jcc.540070216) force field (Figg. S1-S5). Peptides were equilibrated in a water-like environment (dielectric constant set equal to 78.54) or in ethanol (EtOH) (dielectric constant set equal to 24.28), depending on the need. The molecular models were then minimized and equilibrated using Hyperchem 6.01 (Hyperchems, Hypercube, Canada) under constant pressure and temperature (NPT) conditions (pressure = 1 atm, temperature = 298 K). General visualization and imaging of minimized molecular models was performed using VMD 1.9.2 (http://www.ks.uiuc.edu/Research/vmd/).

Receptors synthesis. Tiiii[($3C_3H_7$;$1C_3H_6COOH$),CH_3,Ph] (named **Tiiii**),[27] and **Tiiii[C_3H_7,CH_3,Ph]** (named **Tiiii[2]**)[32] (Fig. 1) were synthesized according to literature procedures.

T-rex synthesis. T-rex beads were synthesized according to the procedure reported by Alessandri.[28] Briefly, monodisperse, 2 μm-sized SiO2 spheres were conformally coated with a 100-nm thick layer of TiO2 by atomic layer deposition (ALD,

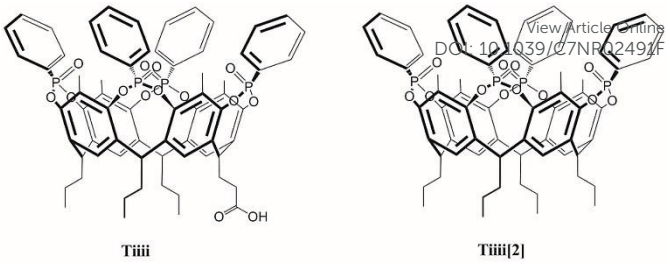

Fig. 1. Molecular structure of **Tiiii** and **Tiiii[2]** cavitands used

Savannah 100, Cambridge Nanotech Inc.) using tetrakis (dimethylamino) titanium(IV) (Sigma Aldrich) and milliQ water as Ti and O precursors, respectively. The as-prepared core/shell beads were annealed in air at 700°C for 4 h. A detailed structural and microstructural characterization is reported in reference 28.

Methylated peptides solutions and peptide-Tiiii molecular recognition. 10^{-3} M solutions of **Tiiii** cavitands in ethanol were obtained by dissolving cavitand powders in pure ethanol (Sigma-Aldrich). Equimolar (10^{-3} M) peptide solutions were obtained by dissolving the different peptide salts (ProteoGenix SAS) in ethanol. The final pH values of **Tiiii** and peptide solutions was 4.5 and 5, respectively.‡ The molecular recognition experiments were carried out by mixing 50 μL of each solution. The mixed solution was stirred at 500 rpm (IKA® MS-3 digital) for one hour at room temperature.

Raman analysis. For each Raman analysis SERS-active 3D colloidal crystals made of self-assembled T-rex beads were infiltrated with 5 μL of the **Tiiii**-peptide complex solution. The same procedure was applied in control experiments. The micro Raman analyses were carried out in backscattering configuration using a Labram HR-800 (Horiba-Jobin Yvon), coupled to an optical microscope (BX41; Olympus Optical Co. Ltd.). All the analyses were carried out using a 632.81 nm HeNe laser as an exciting source (nominal power on the sample surface: 5mW).The baseline of the spectra were corrected with the LabSpec data analysis package. The spectra were acquired from 10 different regions for each sample. The error bars indicate the standard error.

Results and discussion

The experiments were carried out using a small library of five peptides corresponding to the *N*-terminal tail of the histone H3 tail, sketched in panel (a) of Scheme 1. Each peptide consists of a sequence of 15 amino acids *N*-terminated with a 9-fluorenylmethyloxycarbonyl (FMOC) moiety, which serves as protecting and labeling agent. Each peptide bears three lysine residues, located at positions 3, 8 and 13, which from now on will be referred as Lys4, Lys9 and Lys14. An non-methylated peptide was taken as negative control (PC). Three peptides (P1, P2 and P3) bear mono-methylated lysines in different positions: in P1 the methylation is at Lys4, whereas in P2 and P3 the methylation is at Lys9 and Lys14, respectively. Instead, P123 displays all the three lysine residues mono-methylated. According to the energy minimization of the histones

ROYAL SOCIETY OF CHEMISTRY
View Article Online
DOI: 10.1039/C7NR02491F

Nanoscale

ARTICLE

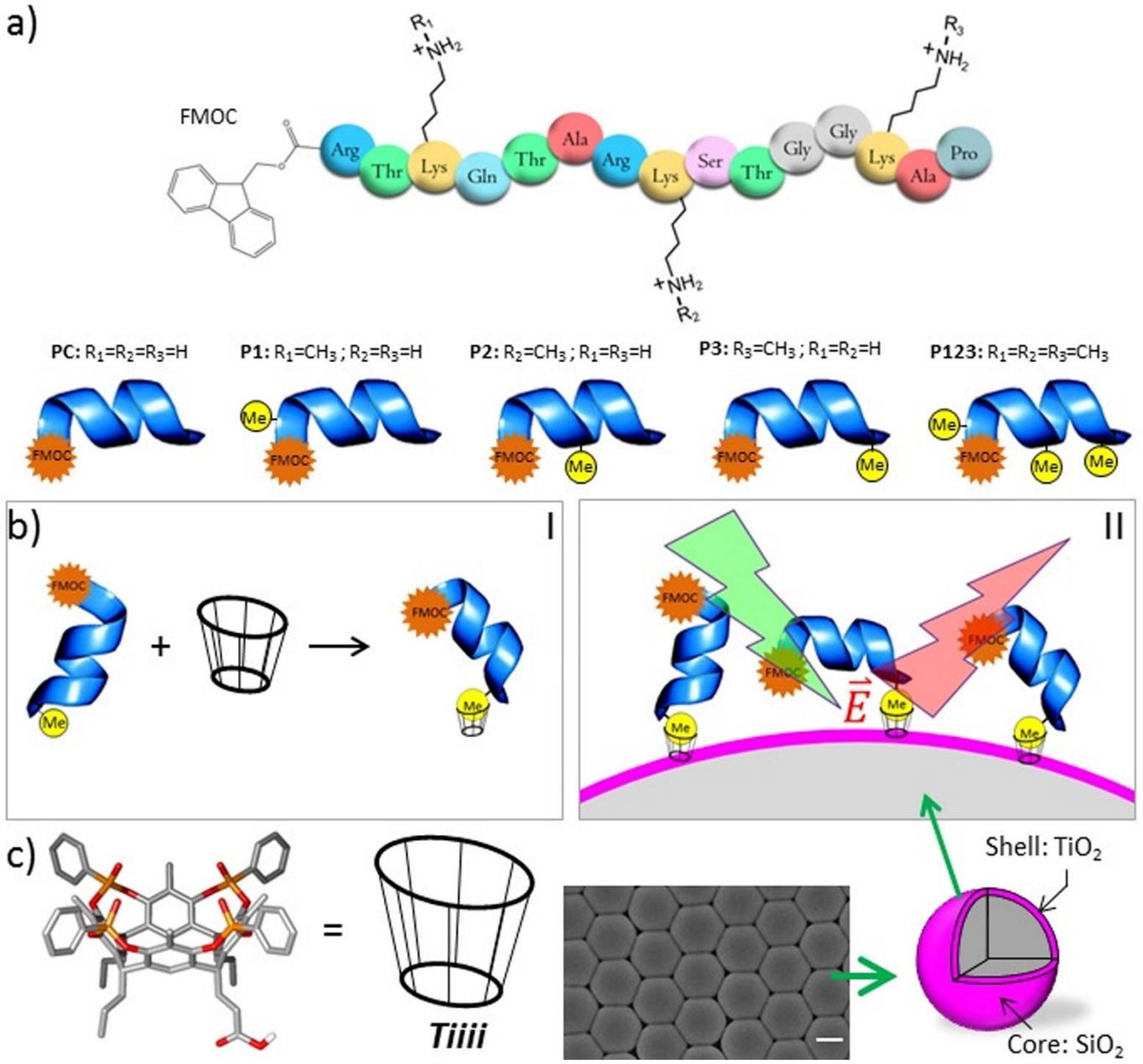

Scheme 1. Materials **(a, c)** and experimental **(b)** design for recognition-separation-probing of lysine mono-methylated histone H3 tail peptides by a supramolecular recognition and T-rex non-plasmonic SERS. For a detailed description refer to the main text. In the SEM image in the bottom left panel the scale bar is 1 μm.

conformations in ethanol (Figg. S1-S5), each peptide presents all lysines side chains free to interact with the **Tiiii** ligand.

The molecular structure of the **Tiiii** ligand equipped with a single carboxylic group at the lower rim is reported in panel (c), as well as a sketch of a single T-rex bead and a SEM image of a portion of one of the 3D colloidal crystals of T-rex beads used as SERS substrates.

The recognition-separation-probing experimental concept is sketched in the (b) panels of Scheme 1. The methylated peptides are captured in ethanol solution by the cavitands,

ROYAL SOCIETY OF CHEMISTRY View Article Online
DOI: 10.1039/C7NR02491F

Nanoscale

ARTICLE

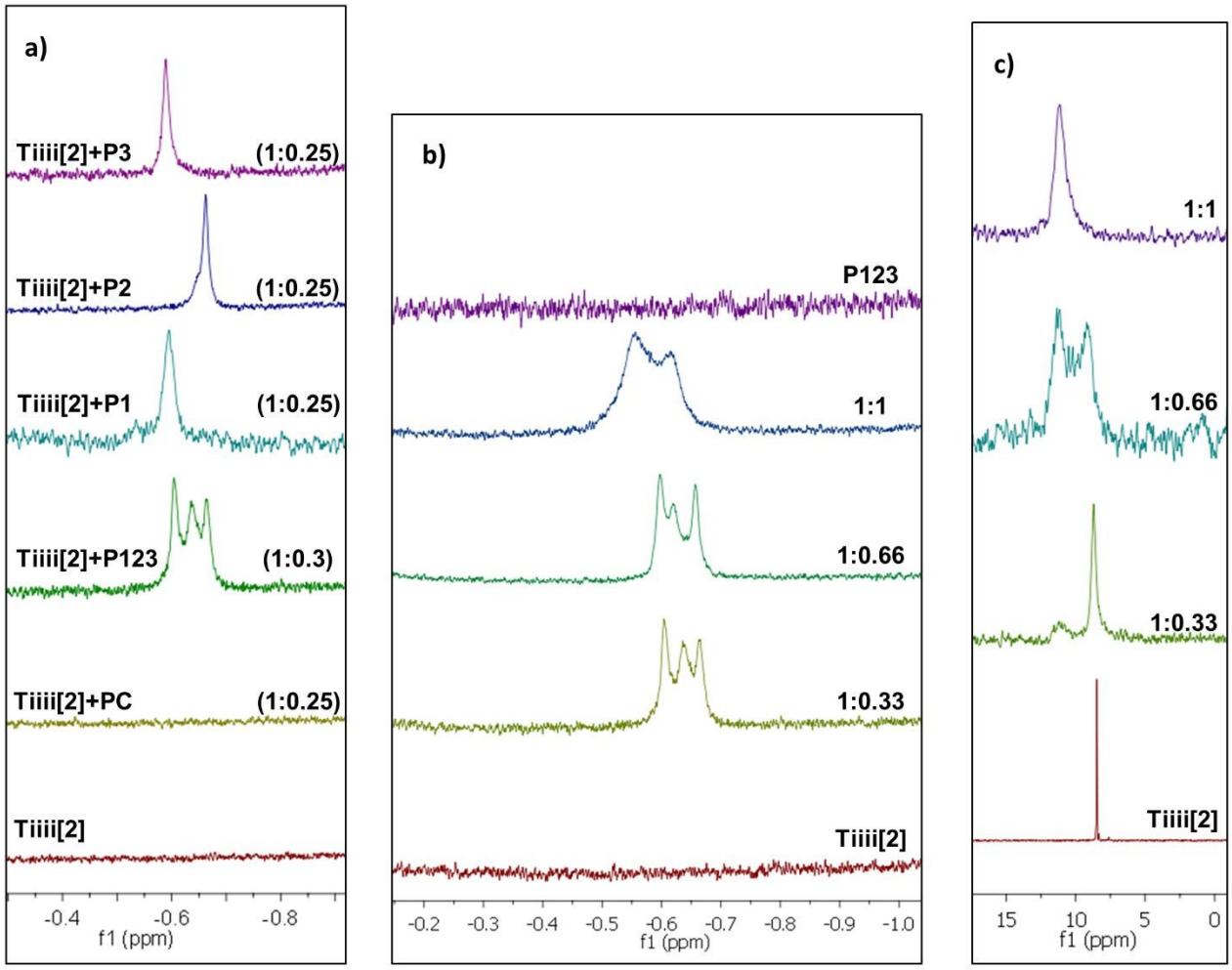

Fig. 2. a) Enlargement of the Lys-NMe$^+$ region related to the ^{1}H NMR spectra (400 MHz, CD_3OD, 298K) of **Tiiii[2]•Peptide** complexes upon addition of 0.25 eq. of P1 (red spectrum), P2 (green spectrum), P3 (violet spectrum) and of 0.3 eq. of P123 (blue spectrum) showing the characteristic upfield shift of the $^+$N-CH_3 resonances. These upfield signals are clearly visible in the presence of an excess of **Tiiii**. b) same enlargement of ^{1}H NMR spectra of the Lys-NMe$^+$ region related to the titration of **Tiiii[2]** with P123: free **Tiiii[C_3H_7, CH_3, Ph]** (**Tiiii[2],** red spectrum, 0.25 eq. and 0.5 eq. of **P123** added (green spectra), the 1:1 complex (blue spectrum) and the free **P123** (violet spectrum). At the correct stoichiometric ratio the $^+$N-CH_3 resonances become too broad to be detected, since the binding of the lysine side chains by the cavitand is under fast chemical exchange at 298 K.[21]. c) the same titration of **Tiiii[2]** with P123 as in b) monitored by ^{31}P NMR.

which selectively bind the Lys-NMe$^+$ moiety forming a stable peptide-cavitand complex (Scheme 1, panel I). The separation of the complexes from the solution and their detection is then performed in one single step by the T-rex bead (panel II). Efficient separation is chemically driven by the cavitand carboxylic group at the lower rim, which chemisorbs onto the T-rex shell by coordinative and ionic bonds with the surface Ti cations.[27] The T-rex substrate has then the additional function to enhance the Raman fingerprint of the complex by non-plasmonic SERS, making it detectable and ensuring at the same time the absence of the complex degradation, typically triggered by plasmonic hot spots (Scheme 1, Panel II).

Solution study. The selective binding of the **Tiiii** ligand to the N-monomethylated peptides was assessed by ^{31}P and ^{1}H NMR titration experiments in methanol-d_4 using the corresponding tetraphosphonate cavitand lacking the carboxylic group at the lower rim (**Tiiii[2]**). The ^{31}P resonance of the **Tiiii[2]** P=O groups moved downfield of about 2.5 ppm in the presence of N-monomethylated peptides (+2.65 ppm for P1, +2.66 ppm for P2, +2.41 ppm for P3 and +2.92 ppm for P123, see Fig. S6-S8-S10-S12). By comparison, the pristine PC moved the P=O signals downfield of only 0.87 ppm (Fig. S14). The corresponding ^{1}H NMR spectra showed an upfield shift of the lysines Lys-NMe$^+$ moieties at negative ppm (−0.60 ppm for P1, -0.66 ppm for P2,

View Article Online
DOI: 10.1039/C7NR03491F

-0.59 ppm for P3, Fig. 2), in a spectral region free of histone resonances (for the complete spectra see Fig. S7-S9-S11-S13-S15). The downfield shift of P=O signals is a clear indication of the participation of the phosphonate groups in protein complexation, whereas the large upfield shift of the methyl residue (more than 3 ppm) is diagnostic of Lys-NMe$^+$ inclusion in the aromatic cavity of the host. Particularly relevant is the spectrum relative to the P123 titration (blue spectrum of Fig. 2), in which all three signals relative to complexed Lys4, Lys9 and Lys14 are present in the range -0.60/-0.66 ppm. It proves that all three monomethylated lysine side chains can be complexed simultaneously by **Tiiii**.

Solid-liquid study. The experiments at the solid-liquid interface were carried out in EtOH, allowing 10^{-3} M solutions of **Tiiii** to interact with 10^{-3} M solutions of peptides ($3\cdot10^{-3}$ M of **Tiiii** in the case of P123, in order to preserve the 1:1 ligand-target stoichiometry) for one hour at room temperature under gentle stirring.‡ The deposition of the **peptide-Tiiii** complexes on the T-rex was obtained by placing a droplet of the solution onto the T-rex substrate and waiting for the solvent to evaporate at ambient conditions. The same solid-liquid adsorption procedure was applied for the experiments aimed at determining the signal background (**Tiiii** alone) and the control experiments (separate peptides and cavitands).

Representative T-rex SERS results and data analysis are shown in Fig. 3a. Data analysis was based on our preliminary results on sensing of mono-methylated lysine protected with Fmoc.[27] We demonstrated that the methylated lysine-**Tiiii** complex can be monitored from the analysis of the Raman modes in the spectral region around 1600 cm^{-1}, which exhibits two distinct Raman peaks, one at 1594 cm^{-1} characteristic of the **Tiiii** aromatic rings and the other around 1608 cm^{-1} originated from the fluorenyl ring of the Fmoc, which labels the methylated lysine.

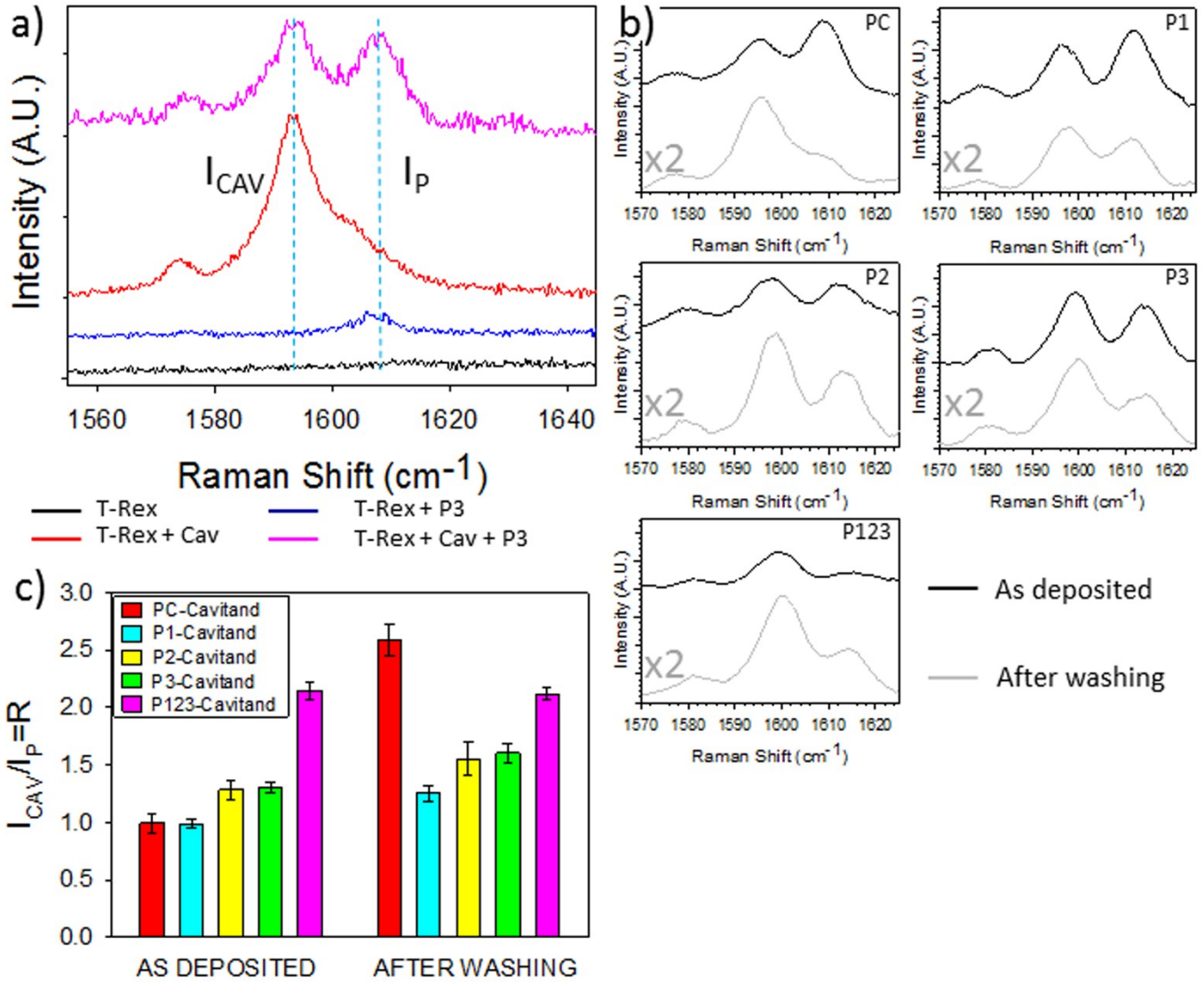

Fig. 3. (a) Representative T-rex SERS fingerprints of the species involved in the experiments: the black spectrum refers to the naked T-rex substrate, the blue one is relative to a given peptide (*e.g.* P3 in the present case) physisorbed onto a T-rex substrate. The red spectrum refers to Tiiii adsorbed on a T-rex substrate. The Raman mode at 1608 cm^{-1} will be utilized as a marker peak to identify the presence of Tiiii receptors. The purple spectrum refers to the same spectral region upon addition of a peptide (*e.g.* P3), indicated by the signal of fluorenyl ring of Fmoc at 1594 cm^{-1}. **(b)** Averaged intensities ratio for the non-methylated and mono-methylated peptides recognized by the cavitand. **(c)** R values of the **P1-Tiiii, P2-Tiiii, P3-Tiiii, P123-Tiiii** and **PC-Tiiii** complexes as adsorbed onto the T-rex substrate and after washing. See the main text for details and Scheme 1 for peptide notation.

ROYAL SOCIETY OF CHEMISTRY View Article Online
DOI: 10.1039/C7NR02491F

Nanoscale

ARTICLE

We followed the same approach to detect the capture and grafting onto the T-rex of methylated peptide by the **Tiiii** and qualitatively evaluating the formed complex stability. It is also important to note that the raw T-rex substrate does not present any Raman mode that interferes in the spectral region of the other species of interest. The purple spectrum of Fig. 3a emphasizes this point by showing the Raman scattering of the **P3-Tiiii** complex, where the expected bands of the **Tiiii** and of the P3 peptide are clearly visible at 1594 cm^{-1} and 1608 cm^{-1}, respectively, and present comparable intensities.

To quantitatively analyze and discuss the data we define a convenient parameter *R,* which represents the ratio between the intensity of the Raman peaks of **Tiiii** and peptide as:

$$R = \frac{I_{CAV}}{I_P}$$

where I_{CAV} and I_P are the Raman peak intensities of **Tiiii** (1594 cm^{-1}) and of the peptide (1608 cm^{-1}), respectively. *R* therefore is directly relates to the relative amount of the **Tiiii** with respect to the peptide on the T-rex surface. The left set of bar charts of Fig. 3c reports the *R* values of the binding partners (namely **P1-Tiiii**, **P2-Tiiii**, **P3-Tiiii**, **P123-Tiiii**, and **PC-Tiiii**) as adsorbed from the solution onto the T-rex substrate ($R_{adsorbed}$), while the right set reports *R* after the adsorbate has been generously rinsed with milliQ water (R_{washed}) (representative raw data are reported in Fig. 3b). Rinsing is performed to wash out non complexed peptides physisorbed onto the T-Rex surface and any possible not chemisorbed **Tiiii** or weakly grafted **peptide-Tiiii** complexes.

It clearly emerges that *R* varies barely for the mono-methylated peptide-**Tiiii** signals before and after washing (blue, yellow and green bars), while it significantly increases for the control non-methylated peptide (**PC-Tiiii**, red bars). These data can be better understood by considering their differential $\Delta R = R_{washed} - R_{adsorbed}$, whose values are reported in Fig. 4a. Their interpretation is sketched in Fig. 4b.

Δ*R* of **PC-Tiiii** is significantly higher than the other signals, meaning that most of the control peptides are removed by rinsing and therefore not recognized and anchored on the T-rex by the **Tiiii**. This agrees with the fact PC does not carry any methylated lysine and cannot be recognized by the **Tiiii**. Instead, all the mono-methylated cases, **P1-Tiiii**, **P2-Tiiii** and **P3-Tiiii**, show markedly lower and equal values of Δ*R*, indicating that a significant amount of the peptides are recognized and anchored by the **Tiiii** to the T-rex surface (note that the **Tiiii** alone resists to rinsing because it is chemisorbed on the T-rex, as shown in reference 27). Remarkably, equal Δ*R* values point to the fact that peptide capture and separation occurs with the same

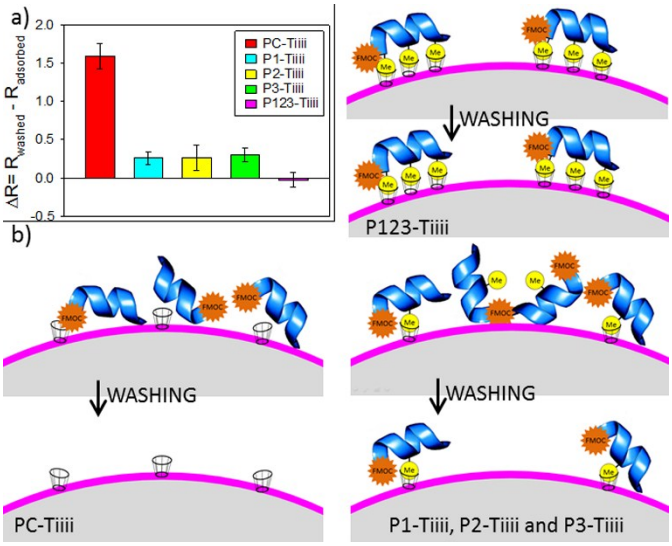

Fig. 4. Recognition, immobilization and signal translation: Panel **(b)** proposes a pictorial interpretation of results summarized in panel **(a)**. See the main text for detailed description.

efficiency to all the three peptides, regardless the position of the methylation.

Finally, Δ*R* of the **P123-Tiiii** results experimentally zero. This means that all the captured P123 from solution is then retained onto the T-Rex after washing. This exceptional performance agrees well with the interaction stoichiometry (three **Tiiii** binding a single peptide), resulting in a more strongly chemisorbed **peptide-Tiiii** complex.

The selectivity of **Tiiii** receptors in binding methylated lysine residues forming stable complexes was then challenged in solutions containing both methylated and non-methylated peptides, which is relevant in view of applications in common protein extracts. Fig. 5a compares Δ*R* values obtained from the recognition-separation-probing experiments performed on the pure solutions of PC and P3 and in equimolar mixed solutions of PC and P3. Δ*R* is increased in the co-presence of both PC and P3 in comparison to that observed for the pure P3 solution. However, it remains significantly lower (1.25 vs. 1.5) than that obtained for the pure P3 control solution. This means that **P3-Tiiii** complexes form and can be separated and detected even in the presence of PC, although the SERS signal lowers because of the halving of the **Tiiii** cavitand complexes. In mixed solutions of P123 and PC (Fig. 5b), the **P123-Tiiii** complex formation and separation is strongly improved (ΔR = 0.4, very close to the value obtained for complexes obtained from pure P123 solutions) in comparison to that observed for P3 and PC mixed solutions, in agreement with results in Fig. 4.

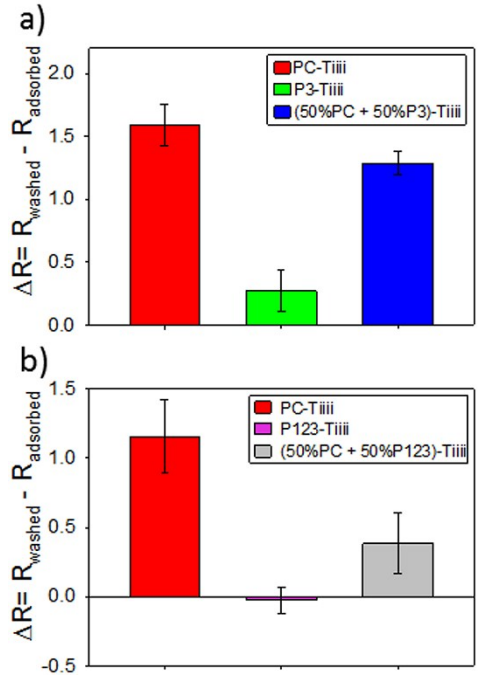

Fig. 5. Selectivity assessment: Comparison between the Δ*R* parameter for pure solutions and a 50% -50 % mixed solution respectively for **(a)** mono-methylated peptide P3 and **(b)** tri-methylated peptide P123.

Conclusions

The unique molecular recognition properties of **Tiiii** and performances of the all-dielectric non-plasmonic resonators T-rex beads were leveraged to provide the first proof of an "all chemical" route for recognition-separation-probing of histone tail peptides presenting mono-methyl modifications of one or more lysines. The developed method performed robustly and with high fidelity with all the tested peptides, regardless the position and number of the modifications. The triple mono-methylated histone P123 is preferentially recognized thanks to the surface multivalency[33-35] of the resulting camouflage.
Such finding and method can turn very useful to improve enrichment and identification of lysine mono-methylated species in mixtures of short peptides obtained from cell lysates by proteolytic fragmentation or other techniques (indeed, working in ethanol may even expose to recognition mono-methylated residues not accessible in aqueous buffers).

Acknowledgements

This work was supported by SUPRANANO (INSTM-Regione Lombardia project). Centro Intefacoltà di Misure "G. Casnati" of the University of Parma is acknowledged for the use of NMR facilities. We thank Matteo Ferroni for support in SEM analysis.

Notes and References

‡ The last step in the histones synthesis is performed in trifluoroacetic acid, therefore all lysines' side chains are already present in the protonated form.

1 S. Lanouette, V. Mongeon, D. Figeys and J. Couture, *Mol. Sys. Biol.*, 2014, **10**, 724.
2 S. M. Carlson and O. Gozani, *J. Mol. Biol.*, 2014, **426**, 3350.
3 J. McGrath and P. Trojer, *Pharmacol. Ther.*, 2015, **150**, 1.
4 H. Huang, S. Lin, B. A. Garcia and Y. Zhao, *Chem. Rev.*, 2015, **115**, 2376.
5 M. Florea, S. Kudithipudi, A. Rei, M. J. Gonzalez-Alvarez, A. Jelttsch and W. M. Nau, *Chem. Eur. J.*, 2012, **12**, 3521.
6 B. D. Strahl, R. Ohba, R. G. Cook and C. David Allis, *Proc. Natl. Acad. Sci. USA*, 1999, **26**, 14967.
7 R. A. Varier and H. T. Timmers, *Biochim. Biophys. Acta*, 2011, **1**, 75.
8 J. Gupta, S. Kumar, J. Li, R. K. Murthy Karuturi and K. Tikoo, *Biochimie,* 2012, **94**, 2656.
9 S. D. Taverna, H. Li, A. J. Ruthenburg, C. D. Allis and D. J. Patel, *Nat. Struct. Mol. Biol.*, 2007, **14**, 1025.
10 S. A. Jacobs and S. Khorasanizadeh, *Science*, 2002, **295**, 2080.
11 S. A. Minaker, K. D. Daze, M. C. F. Ma and F. Hof, *J. Am. Chem. Soc.*, 2012, **134**, 11674.
12 D. Bier, R. Rose, K. Bravo-Rodriguez, M. Bartel, J. M. Ramirez-Anguita, S. Dutt, C. Wilch, F.-G. Klärner, E. Sanchez-Garcia, T. Schrader and C. Ottmann, *Nat. Chem.*, 2013, **5**, 234.
13 K. D. Daze and F. Hof, *Acc. Chem. Res.*, 2013, **46**, 937.
14 M. Mallon, S. Dutt, T. Schrader and P. B. Crowley, *Chem. Bio. Chem.*, 2016, **17**, 774.
15 R. E. McGovern, B. D. Snarr, J. A. Lyons, J. McFarlane, A. L. Whiting, I. Paci, F. Hof and P. B. Crowley, *Chem. Sci.*, 2015, **6**, 442.
16 C. S. Beshara, C. E. Jones, K. D. Daze, B. J. Lilgert and F. Hof, *Chem. Bio. Chem.*, 2010, **11**, 63.
17 L. A. Ingerman, M. E. Cuellarb and M. L. Waters, *Chem. Commun.*, 2010, **46**, 1839.
18 M. A. Gamal-Eldin and D. H. Macartney, *Org. Biomol. Chem.*, 2013, **11**, 488.
19 R. Pinalli, M. Suman and E. Dalcanale, *Eur. J. Org. Chem.*, 2004, 451.
20 R. Pinalli and E. Dalcanale, *Acc. Chem. Res.*, 2013, **46**, 399.
21 R. Pinalli, G. Brancatelli, A. Pedrini, D. Menozzi, D. Hernández, P. Ballester, S. Geremia and E. Dalcanale, *J. Am. Chem. Soc.*, 2016, **138**, 8569.
22 D. A. Dougherty, *Acc. Chem. Res.*, 2013, **46**, 885.
23 M. Dionisio, G. Oliviero, D. Menozzi, S. Federici, R. M. Yebeutchou, F. P. Schmidtchen, E. Dalcanale and P. Bergese, *J. Am. Chem. Soc.*, 2012, **134**, 2392.
24 A. Norouzy, Z. Azizi and W. M. Nau, *Angew. Chem. Int. Ed.*, 2015, **54**, 792.
25 G. Ghale and W. N. Nau, *Acc. Chem. Res.*, 2014, **47**, 2150.
26 Y. Liu, L. Perez, M. Mettry, C. J. Easley, R. J. Hooley and W. Zhong, *J. Am. Chem. Soc.*, 2016, **138**, 10746.
27 I. Alessandri, E. Biavardi, A. Gianoncelli, P. Bergese and E. Dalcanale, *ACS Appl. Mater. Interfaces*, 2016, **8**, 14944.
28 I. Alessandri, *J. Am. Chem. Soc.*, 2013, **135**, 5541.
29 I. Alessandri and L. E. Depero, *Small*, 2014, **10**, 1294.
30 N. Bontempi, L. Carletti, C. De Angelis and I. Alessandri, *Nanoscale*, 2016, **8**, 3226.
31 I. Alessandri and J. R. Lombardi, *Chem. Rev.*, 2016, **116**, 14921.
32 E. Biavardi, G. Battistini, M. Montalti, R. M. Yebeutchou, L. Prodi and E. Dalcanale, *Chem. Commun.*, 2008, 1638.
33 A. Mulder, J. Huskens and D. N. Reinhoudt, *Org. Biomol. Chem.*, 2004, **2**, 3409.
34 J. Huskens, A. Mulder, T. Auletta, C. A. Nijhuis, M. J. Ludden and D. N. Reinhoudt, *J. Am. Chem. Soc.*, 2004, **126**, 6784.
35 R. Valiokas, G. Klenkar, A. Tinazli, R. Tampe, B. Liedberg and J. Piehler, *Chem. Bio. Chem.*, 2006, **7**,1325.